

King's Research Portal

DOI:

[10.1093/brain/awab118](https://doi.org/10.1093/brain/awab118)

Document Version

Peer reviewed version

[Link to publication record in King's Research Portal](#)

Citation for published version (APA):

Eyre, M., Fitzgibbon, S. P., Ciarrusta, J., Cordero-Grande, L., Price, A. N., Poppe, T., Schuh, A., Hughes, E., O'Keeffe, C., Brandon, J., Cromb, D., Vecchiato, K., Andersson, J., Duff, E. P., Counsell, S. J., Smith, S. M., Rueckert, D., Hajnal, J. V., Arichi, T., ... Edwards, A. D. (2021). The Developing Human Connectome Project: typical and disrupted perinatal functional connectivity. *Brain : a journal of neurology*.
<https://doi.org/10.1093/brain/awab118>

Citing this paper

Please note that where the full-text provided on King's Research Portal is the Author Accepted Manuscript or Post-Print version this may differ from the final Published version. If citing, it is advised that you check and use the publisher's definitive version for pagination, volume/issue, and date of publication details. And where the final published version is provided on the Research Portal, if citing you are again advised to check the publisher's website for any subsequent corrections.

General rights

Copyright and moral rights for the publications made accessible in the Research Portal are retained by the authors and/or other copyright owners and it is a condition of accessing publications that users recognize and abide by the legal requirements associated with these rights.

- Users may download and print one copy of any publication from the Research Portal for the purpose of private study or research.
- You may not further distribute the material or use it for any profit-making activity or commercial gain
- You may freely distribute the URL identifying the publication in the Research Portal

Take down policy

If you believe that this document breaches copyright please contact librarypure@kcl.ac.uk providing details, and we will remove access to the work immediately and investigate your claim.

The Developing Human Connectome Project: typical and disrupted perinatal functional connectivity

Michael Eyre^a, Sean P Fitzgibbon^b, Judit Ciarrusta^{a,c}, Lucilio Cordero-Grande^a, Anthony N Price^a, Tanya Poppe^a, Andreas Schuh^d, Emer Hughes^a, Camilla O’Keeffe^a, Jakki Brandon^a, Daniel Cromb^a, Katy Vecchiato^{a,c}, Jesper Andersson^b, Eugene P Duff^{b,e}, Serena J Counsell^a, Stephen M Smith^b, Daniel Rueckert^d, Joseph V Hajnal^a, Tomoki Arichi^{a,f}, Jonathan O’Muircheartaigh^{a,c}, Dafnis Batalle^{a,c,†*}, A David Edwards^{a,†*}

^a Centre for the Developing Brain, School of Biomedical Engineering & Imaging Sciences, King's College London, London, UK

^b Wellcome Centre for Integrative Neuroimaging (WIN FMRIB), University of Oxford, Oxford, UK

^c Department of Forensic and Neurodevelopmental Science, Institute of Psychiatry, Psychology and Neuroscience, King's College London, London, UK

^d Biomedical Image Analysis Group, Imperial College London, London, UK

^e Department of Paediatrics, University of Oxford, Oxford, UK

^f Department of Bioengineering, Imperial College London, London, UK

†These authors contributed equally

*Corresponding authors:

Dr. Dafnis Batalle
Department of Forensic and Neurodevelopmental Science
Institute of Psychiatry, Psychology & Neuroscience
King's College London
16, De Crespigny Park, SE5 8AF, London, UK
+44-(0)-207-848-0922 | dafnis.batalle@kcl.ac.uk

Professor David Edwards
Centre for the Developing Brain
School of Biomedical Engineering & Imaging Sciences
King's College London
+44-(0)-207-188-9158 | ad.edwards@kcl.ac.uk

Abstract

The Developing Human Connectome Project (dHCP) is an Open Science project which provides the first large sample of neonatal functional MRI (fMRI) data with high temporal and spatial resolution. This data enables mapping of intrinsic functional connectivity between spatially distributed brain regions under normal and adverse perinatal circumstances, offering a framework to study the ontogeny of large-scale brain organisation in humans. Here, we characterise in unprecedented detail the maturation and integrity of resting-state networks (RSNs) at term-equivalent age in 337 infants (including 65 born preterm).

First, we applied group independent component analysis (ICA) to define 11 RSNs in term-born infants scanned at 43.5-44.5 weeks postmenstrual age (PMA). Adult-like topography was observed in RSNs encompassing primary sensorimotor, visual and auditory cortices. Among six higher-order, association RSNs, analogues of the adult networks for language and ocular control were identified, but a complete default mode network precursor was not. Next, we regressed the subject-level datasets from an independent cohort of infants scanned at 37-43.5 weeks PMA against the group-level RSNs to test for the effects of age, sex and preterm birth. Brain mapping in term-born infants revealed areas of positive association with age across four of six association RSNs, indicating active maturation in functional connectivity from 37 to 43.5 weeks PMA. Female infants showed increased connectivity in inferotemporal regions of the visual association network. Preterm birth was associated with striking impairments of functional connectivity across all RSNs in a dose-dependent manner; conversely, connectivity of the superior parietal lobules within the lateral motor network was abnormally increased in preterm infants, suggesting a possible mechanism for specific difficulties such as developmental coordination disorder which occur frequently in preterm children.

Overall, we find a robust, modular, symmetrical functional brain organisation at normal term age. A complete set of adult-equivalent primary RSNs is already instated, alongside emerging connectivity in immature association RSNs, consistent with a primary-to-higher-order ontogenetic sequence of brain development. The early developmental disruption imposed by preterm birth is associated with extensive alterations in functional connectivity.

Introduction

The Developing Human Connectome Project (dHCP) is an Open Science project funded by the European Research Council to provide a large dataset of functional and structural brain images from 20 to 44 weeks of gestational age (GA). This enables the characterisation of 4-dimensional (three spatial dimensions and time) connectivity maps, which map the trajectories of human brain development to improve understanding of normal development and allow earlier detection and intervention for neurological and psychological disorders.

This paper analyses functional connectivity at the time of normal birth in infants born at term and preterm. Temporal coherences in the blood-oxygen–level-dependent (BOLD) contrast measured with resting-state functional magnetic resonance images (rs-fMRI) can be spatiotemporally decomposed into resting-state networks (RSNs) (Damoiseaux *et al.*, 2006) (Biswal *et al.*, 1995), predominantly at low frequency (< 0.1 Hz) (Cordes *et al.*, 2001), distinct from cardiovascular signal (De Luca *et al.*, 2006). Whilst RSNs have been extensively and robustly characterized in the mature brain, previous studies of RSN development in newborn infants have been limited by smaller sample sizes. The dHCP provides the first high-quality, large-scale, 4-dimensional dataset of functional connectivity at this critical period of development, enabling us to address two key questions. Firstly, are higher-order RSNs such as the default-mode network (DMN) (Raichle *et al.*, 2001) instated with adult topology in the neonatal period? Some find analogues of these at term-equivalent age (TEA) (Doria *et al.*, 2010; Fransson *et al.*, 2009; Fransson *et al.*, 2007; Smyser *et al.*, 2010; Smyser *et al.*, 2016) while others locate their origin in later infancy or early childhood, contemporaneous with the emergence of the higher cognitive abilities these networks are believed to support (Gao *et al.*, 2014; Gao *et al.*, 2015). Secondly, what is the effect of preterm birth on RSN development? Preterm birth is associated with significant risk for enduring neurodevelopmental and psychiatric problems in later life (Bhutta *et al.*, 2002; Marlow *et al.*, 2005; Saigal and Doyle, 2008; Nosarti *et al.*, 2012), even in the absence of overt structural brain injury during the preterm period. Various alterations in the complexity, scope, strength and efficiency of functional connectivity in preterm-at-term infants have been reported (Smyser *et al.*, 2010; Toulmin *et al.*, 2015; Ball *et al.*, 2016; Smyser *et al.*, 2016; Bouyssi-Kobar *et al.*, 2019); however, the majority of studies lack the large numbers of control subjects required to characterise these effects with precision.

The mature adult RSNs are well characterised, with high intra-subject reproducibility (Finn *et al.*, 2015; Wang *et al.*, 2015), largely consistent topology across healthy subjects, and anatomical mapping that reinforces both structural and task-fMRI-derived parcellations of the cortex (Glasser *et al.*, 2016). The identification of fMRI-RSN signatures associated with

disease offers considerable translational potential due to rs-fMRI's relatively straightforward and widely-used acquisition, whole-brain coverage, and high spatial resolution compared to other functional imaging methods. The achievement of this in the immature brain requires a complete account of RSN ontogeny. The developing CNS shows spontaneous, patterned, correlated intrinsic activity from early prenatal life (reviewed in Blankenship and Feller, 2010; Keunen et al., 2017; Vasung et al., 2019); immature RSNs can be identified from as early as 26 weeks postmenstrual age (PMA) in the preterm infant (Doria et al., 2010; Smyser et al., 2010). By TEA, RSNs encompassing brain regions serving primary functions (sensorimotor, auditory, visual) are clearly apparent in mature configuration in both term and preterm-born infants (Doria et al., 2010; Fransson et al., 2011; Fransson et al., 2009; Fransson et al., 2007; Gao et al., 2014; Gao et al., 2015; Smyser et al., 2016) and show minimal change in infancy, while higher-order association networks appear to be largely fragmented at TEA, with studies suggesting that they synchronise into complete adult-like core structure in the first year (DMN, dorsal attention network) or second year (salience network, bilateral frontoparietal networks) of life (Gao *et al.*, 2014; Gao *et al.*, 2015). Importantly, TEA is not a single timepoint but rather a window encompassing a critical period of brain development in which there is intense myelination of white matter (reviewed in Dubois et al., 2014) and rapid expansion in both the size and gyrification of the cerebral cortex (Dubois et al., 2019; Shimony et al., 2016). Dense sampling across the age range is therefore required to map the associated changes in functional connectivity.

Here we apply a data-driven approach to 337 rs-fMRI datasets acquired in term and preterm infants between 37 and 44.5 weeks PMA. We first defined a normative set of RSNs in a subsample of term-born infants scanned at 43.5-44.5 weeks PMA using probabilistic independent component analysis (ICA) (Beckmann and Smith, 2004). ICA is a dimensionality reduction technique which decomposes data into a set of components with maximal statistical independence; applied to rs-fMRI, ICA can reveal large-scale brain networks without requirement for a predefined model of network structure. We then regressed subject-level data from term and preterm infants scanned at 37-43.5 weeks PMA against these networks. The resulting whole-brain correlation maps enabled us to both characterise the ontogeny of individual RSNs, and investigate the influence of prematurity on cortical functional connectivity. We hypothesised that primary sensorimotor RSNs would be well established at TEA, while higher-order RSNs would be immature and emerging; and that preterm birth would be associated with reduced functional connectivity at TEA.

Materials and methods

Subjects

Research participants were prospectively recruited as part of the dHCP, an observational, cross-sectional Open Science programme approved by the UK National Research Ethics Authority (14/LO/1169). Written consent was obtained from all participating families prior to imaging. Term-born infants were recruited from the postnatal wards and approached on the basis of being clinically well. Preterm-born infants were recruited from the neonatal unit and postnatal wards. Infants were not approached for study inclusion if there was a history of severe compromise at birth requiring prolonged resuscitation, a diagnosed chromosomal abnormality or any contraindication to MRI scanning (e.g., due to incompatible implants). No infants included in the final study group required treatment for clinically significant brain injury. We selected 416 structural-functional datasets acquired at TEA from the 2019 (second) dHCP data release. Only infants scanned at 37-44.5 weeks PMA in term-born infants, or 37-43.5 weeks PMA in preterm-born infants, were considered for inclusion. One infant was included twice due to two datasets being acquired at different ages; only the second dataset was used. Thirty-five infants were excluded due to a history of neurodevelopmental disorder in a first-degree relative. Forty-three were excluded due to motion (see **Functional data pre-processing**). The final study population therefore consisted of 337 infants, divided into three groups: term-born infants scanned at 43.5-44.5 weeks PMA, who were used to define the normative set of RSNs and excluded from all subsequent subject-level analyses (i); and the remaining infants scanned at 37-43.5 weeks PMA, including both term-born (ii) and preterm-born (iii) infants (**Table 1**). No infants in the preterm study group had major brain injury such as periventricular leukomalacia, grade 3 or 4 intraventricular haemorrhage, major intracerebral haemorrhage, or ischaemic focal brain lesions. As is commonly seen in preterm infants there was evidence of mild pathologies including 15 (23%) with a history of grade 1 or 2 IVH; 10 (15%) with small cerebellar haemorrhage with no involvement of the vermis; 22 (34%) with punctate white matter lesions; and 22 (34%) with diffuse excessively high signal intensity (DEHSI) of the white matter. These mild pathologies are known to be poorly predictive of later neurodevelopmental outcome at the individual level (O'Shea et al., 2012; Steggerda et al., 2013; Kersbergen et al., 2014; Broström et al., 2016), and there were no significant differences in early developmental outcome between the term and preterm-born groups (**Table 1**).

MR data acquisition

Neuroimaging was acquired in a single scan session for each infant at the Evelina Newborn Imaging Centre, Evelina London Children's Hospital, using a 3-Tesla Philips Achieva system (Philips Medical Systems, Best, The Netherlands). All infants were scanned without sedation in a scanner environment optimized for safe and comfortable neonatal imaging, including a dedicated transport system, positioning device and a customized 32-channel receive coil, with a custom-made acoustic hood (Hughes et al., 2017). MR-compatible ear putty and earmuffs were used to provide additional acoustic noise attenuation. Infants were fed, swaddled and comfortably positioned in a vacuum jacket prior to scanning to promote natural sleep. All scans were supervised by a neonatal nurse and/or paediatrician who monitored heart rate, oxygen saturation and temperature throughout the scan.

High-temporal-resolution BOLD fMRI optimized for neonates was acquired over 15 minutes 3 seconds (2300 volumes) using a multislice gradient-echo echo planar imaging (EPI) sequence with multiband excitation (multiband factor 9). Repetition time (TR) was 392 milliseconds, echo time (TE) was 38 milliseconds, flip angle was 34° , and the acquired spatial resolution was 2.15 mm isotropic (Price et al., 2015). For registration of the fMRI data, high-resolution T1- and T2-weighted anatomical imaging was also acquired in the same scan session, with a spatial resolution of 0.8 mm isotropic (T1w: field of view $145 \times 122 \times 100$ mm, TR 4795 ms; T2w: field of view $145 \times 145 \times 108$ mm, TR 12000 ms, TE 156 ms).

Functional data pre-processing

Data were pre-processed using an in-house pipeline optimized for neonatal imaging and specifically developed for the dHCP, detailed in Fitzgibbon et al. (2020). In brief, susceptibility dynamic distortion together with intra- and inter-volume motion effects were corrected in each subject using a bespoke pipeline including slice-to-volume and rigid-body registration (Andersson et al., 2018; Andersson et al., 2017; Andersson et al., 2001; Andersson et al., 2003). In order to regress out signal artifacts related to head motion, cardiorespiratory fluctuations and multiband acquisition (Salimi-Khorshidi et al., 2014), 24 extended rigid-body motion parameters were regressed together with single-subject ICA noise components identified with the FSL FIX tool (Oxford Centre for Functional Magnetic Resonance Imaging of the Brain's Software Library, version 5.0). Denoised data were registered into T2w native space using boundary-based registration (Greve and Fischl, 2009) and non-linearly registered to a standard space based on a weekly template from the dHCP volumetric atlas (Schuh et al., 2018) using a diffeomorphic multimodal (T1/T2) registration (Avants et al., 2008).

While the fMRI preprocessing pipeline for the dHCP (Fitzgibbon et al., 2020) addresses the potential problem of head motion in rs-fMRI data (Power et al., 2012; Satterthwaite et al., 2012), motion is also a surrogate marker of the arousal state of the infant, which interacts with the underlying neural activity (Denisova, 2019; Whitehead et al., 2018). To address this issue, we opted for a conservative approach consisting in the selection of a continuous sub-sample of the data (~70%) with lowest motion for each subject, and excluding those subjects with a high level of motion from further analyses. Specifically, volumes with DVARS (the root mean square intensity difference between successive volumes) higher than 1.5 IQR above the 75th centile, after motion and distortion correction, were considered as motion outliers (Fitzgibbon et al., 2020). Mean DVARS was 90.5 (SD 18.5) in the term-born group and 95.5 (SD 20.3) in the preterm-born group ($p = 0.056$, unpaired t-test). As DVARS is a relative measure, the absolute DVARS cutoff varied between subjects. Within each acquired dataset (2300 volumes), the continuous set of 1600 volumes with the minimum number of motion-outlier volumes was identified, and the dataset cropped accordingly for all subsequent analyses. Subjects with more than 160 motion-outlier volumes (10% of the cropped dataset) were excluded entirely. This allowed us to minimise the potential effect of different states of arousal even after appropriately denoising the data. The number of motion-outlier volumes remaining in the cropped dataset was recorded for each subject and included as a covariate in all subsequent regression analyses. The median number of motion-outlier volumes in the term-born group was 49.5 (IQR 27-86.5) and in the preterm-born group was 34 (IQR 12-83) (group difference not significant under assumption of normality [$p = 0.185$, unpaired t-test] or non-normality [$p = 0.052$, Mann-Whitney U test]).

Functional data analysis

Group-level network definition

We first defined the normative set of RSNs by group ICA in 24 healthy term-born infants scanned at 43.5-44.5 weeks PMA. These subjects were excluded from all subsequent regression analyses. Probabilistic group ICA by temporal concatenation across subjects was carried out using FSL MELODIC (Beckmann and Smith, 2004). The ICA dimensionality was set at 30, representing a pragmatic balance between robustness and interpretability (as in (Toulmin et al., 2015)). The output comprised 30 group-average spatial maps representing 30 independent components. The maps were visually inspected and each component manually labelled as RSN or noise, following guidelines in Fitzgibbon et al. (2020).

Subject-level analyses

We next regressed the group-level spatial maps into the subject-level 4D space-time datasets of the subjects scanned at 37-43.5 weeks PMA (248 term-born, 65 preterm-born). Specifically, the group-level spatial maps (including both RSN signal and artifact components) were used to generate subject-specific versions of the spatial maps and associated time series using dual regression (Nickerson et al., 2017). Artifact components were included to better account for confound variance (noise) in the regression model (Beckmann *et al.*, 2009). First, for each subject, the set of group-level RSN spatial maps was regressed (as spatial regressors in a multiple regression) into the subject's 4D space-time dataset. This resulted in a set of subject-specific time series, one per group-level spatial map. Next, those timeseries were regressed (as temporal regressors, again in a multiple regression) into the same 4D dataset, resulting in a set of subject-specific spatial maps, one per group-level spatial map.

We then performed cross-subject analysis using general linear models (GLM) to test for the effects of group (term vs. preterm birth, sex) and continuous variables (GA at birth, PMA at scan) on the subject-level RSN spatial maps, including the number of motion-compromised volumes as a nuisance covariate. Specifically, in the model evaluating the effect of PMA at scan (term-born infants only) the covariates were sex and motion; in the model evaluating the effect of sex the covariates were PMA at scan, GA at birth and motion; in the model evaluating the effect of term vs. preterm birth the covariates were PMA at scan, sex and motion; and in the model evaluating the effect of GA at birth the covariates were PMA at scan, sex and motion. A further group-level analysis was conducted in which term-born infants were separated into weekly bins according to their PMA at scan, enabling group-average maps of functional connectivity at each week of brain development to be generated for qualitative comparison. For this we entered data from the 20 subjects in each bin (37.5-38.5 weeks, 38.5-39.5 weeks, 39.5-40.5 weeks, 40.5-41.5 weeks, 41.5-42.5 weeks) with the lowest number of postnatal days of life at time of scan, to maximise similarity between groups for meaningful visual comparison. The covariates in this model were sex and motion. Voxel-wise statistical tests were implemented in FSL *randomise* (Winkler et al., 2014) using threshold-free cluster enhancement (Smith and Nichols, 2009) with 5000 permutations. As all contrasts were two-tailed, family-wise error-rate (FWE) corrected (for multiple comparisons across voxels) p-values less than 0.025 were accepted as significant. Due to the exploratory nature of this study the main results are presented without correction for the effect of multiple RSNs assessed, however we also provide the Bonferroni-corrected results (i.e. $p < 0.025 / n$ RSNs)) as supplementary figures.

To further quantify longitudinal changes in within-network functional connectivity, we analysed the relationship between PMA at scan and a derived parameter we term ‘core network strength’. This measure was determined for each RSN for each subject by masking the RSN-specific spatial map (the output of stage two of dual regression) by the corresponding group-ICA network template thresholded at $Z > 3$, then calculating the mean β parameter value (regression coefficient) within the masked image. The partial Spearman’s correlation between core network strength and PMA at scan was calculated in term-born infants while controlling for sex and motion (number of motion-compromised volumes), and a GLM was used to test for group differences in core network strength between term and preterm infants while controlling for PMA at scan, sex and motion. Correlation and GLM analyses of core network strength were implemented in Python 3.7 with *pingouin* 0.2.9 and *statsmodels.api* 0.10.1.

Anatomical localisation and data visualisation

Results were localised in the standard space using an in-house adaptation of the neonatal version (Shi et al., 2011) of the AAL atlas (Tzourio-Mazoyer et al., 2002), projected to the 40-week high-resolution neonatal dHCP template (Schuh et al., 2018).

Data were displayed using *FSLeyes* for planar visualisation and Connectome Workbench for cortical surface visualisation.

Data availability

The dHCP is an open-access project. The imaging and collateral data used in this study were included in the 2019 (second) dHCP data release, which can be downloaded by registering at <https://data.developingconnectome.org/>

Results

Resting-state networks

Eleven RSNs were identified by group ICA in a sub-sample of term-born infants scanned between 43.5 and 44.5 weeks PMA ($n = 24$), who were excluded from any further analyses. Five RSNs included primary motor or sensory cortical areas and were categorised as primary networks (**Fig. 1A**): medial motor, lateral motor, somatosensory, auditory and visual. The

remaining six were categorised as association networks (**Fig. 1C**): motor association (including the premotor and supplementary motor areas), temporoparietal (including Broca's area and the extended Wernicke's area), posterior parietal (including the precuneus and posterior cingulate cortices), frontoparietal (including the frontal, supplementary and parietal eye fields), prefrontal and visual association. The full cortical surface parcellation is provided in **Supplementary Fig. S1** and the **Supplementary Video**.

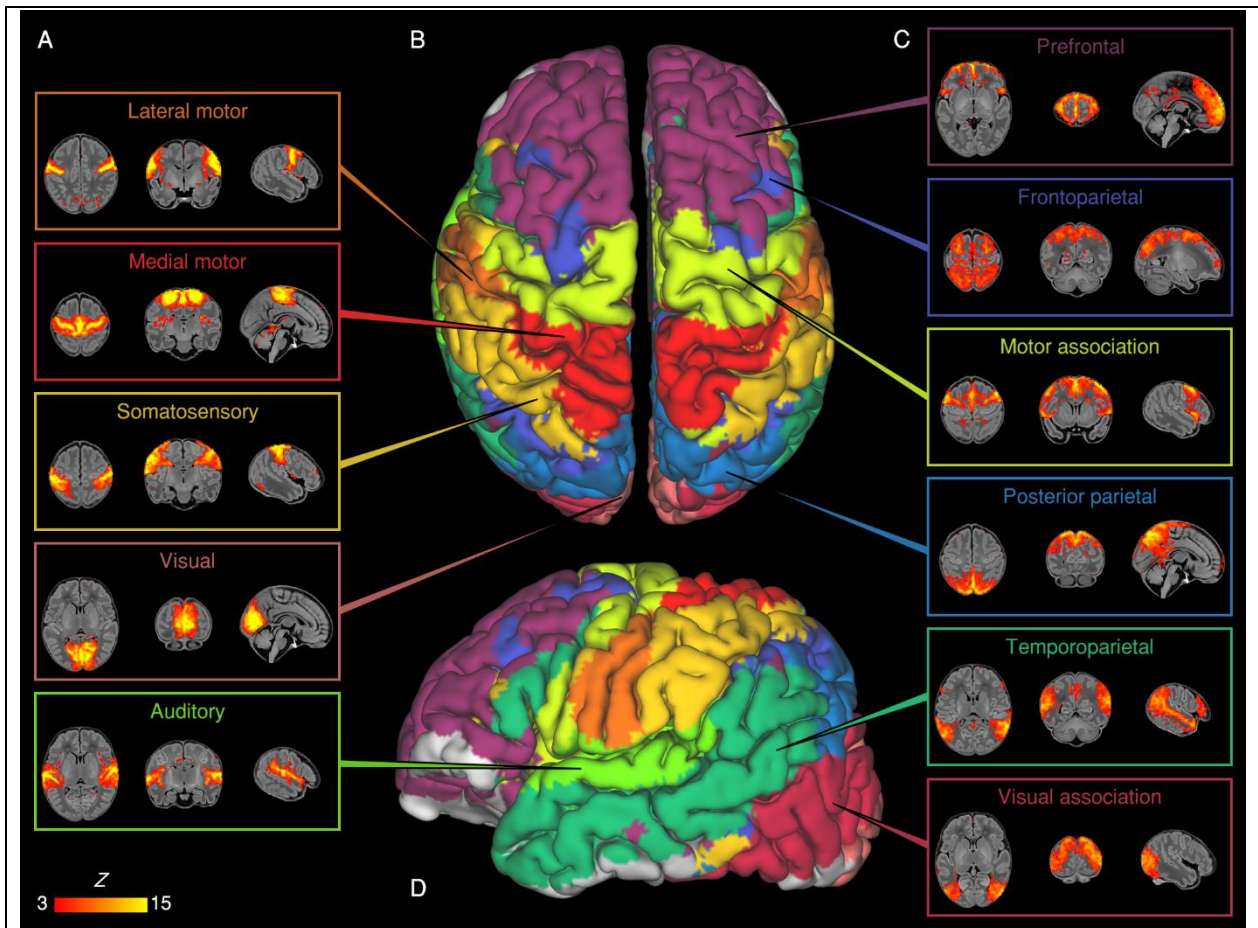


Figure 1. Resting-state networks identified by group independent component analysis. Spontaneous BOLD activity patterns (RSNs) derived from group ICA in 24 term-born infants scanned at 43.5-44.5 weeks PMA. Panels: Example axial, coronal, and sagittal slices for meaningful spatial patterns in primary (A) and association (C) RSNs, thresholded at $Z > 3$ and overlaid on a T1 structural template, displayed in radiological convention. Centre: Functional parcellation of the brain using a 'winner-takes-all' approach based on the RSNs from group ICA. RSNs were spatially smoothed and thresholded at $Z > 1$ prior to determination of the 'winning' RSN at each voxel. The resulting volume was projected to the midthickness cortical surface using enclosed (nearest neighbour) volume-to-surface mapping, here displayed on the pial surface of an individual subject scanned at 42 weeks PMA and viewed from the dorsal (B) and left lateral (D) aspects.

Effect of postmenstrual age at scan

To characterise normal maturation in functional connectivity from 37-43.5 weeks in term-born infants, we analysed the association between previously calculated RSNs independently regressed to each subject and PMA at scan, while controlling for sex and motion. Brain regions showing increasing connectivity with older PMA at scan were identified in four RSNs, all association networks (**Fig. 2**; Bonferroni-corrected, **Supplementary Fig. S2**). Localisation of significant voxels to the AAL atlas is provided in the **Supplementary Table S1**. There were no brain tissue regions showing negative association with older age at scan.

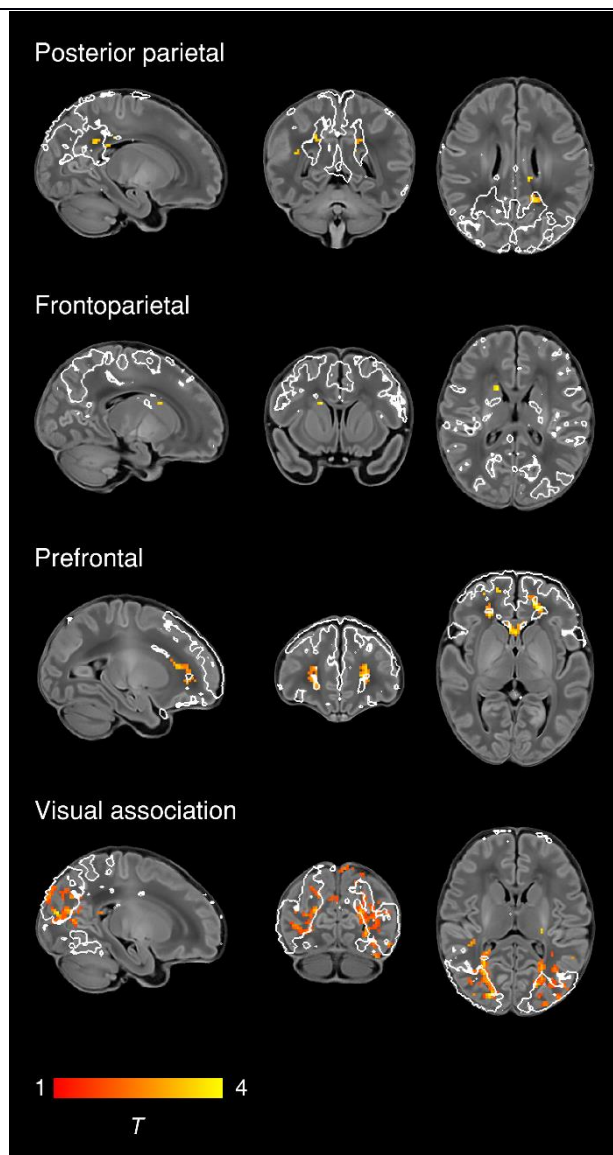


Figure 2. Changes in network shape with increasing age at scan. Brain regions showing increasing functional connectivity with older PMA at scan in term-born infants scanned at 37-43.5 weeks PMA. Example sagittal, coronal, and axial slices for meaningful spatial patterns in four RSNs are shown, overlaid on a T1 structural template and displayed in radiological convention. T-statistic maps were thresholded at $p < 0.025$ (FWE corrected). White lines represent the outlines of the group-ICA RSNs, thresholded at $Z > 3$.

To further illustrate maturational changes in functional connectivity, we produced spatial maps of average network structure in term-born infants categorised into weekly groups according to their PMA at scan, while controlling for sex and motion (**Fig. 3**).

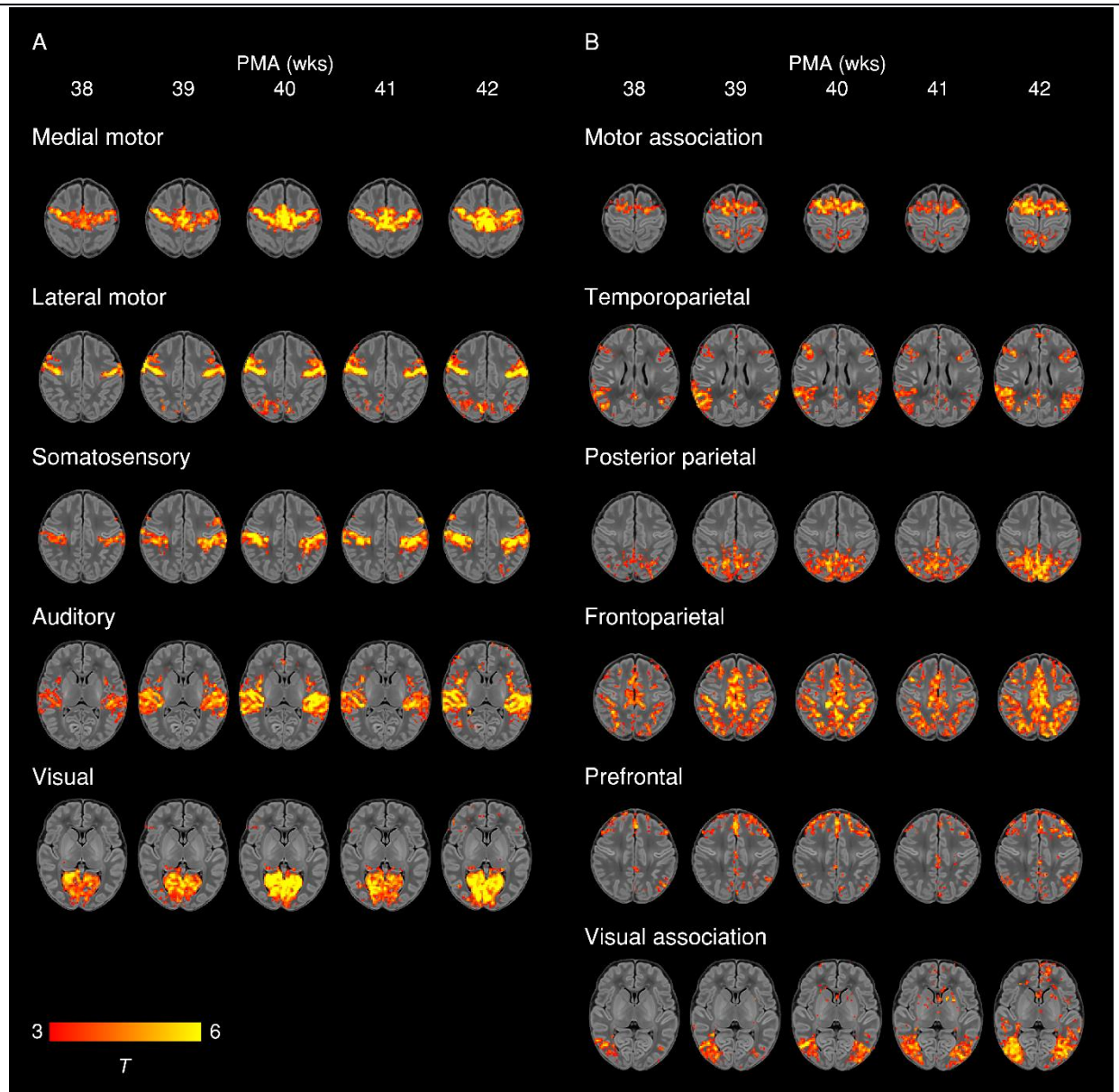


Figure 3. Weekly maturation in functional network structure at term-equivalent age. Group-average *t*-statistic maps of functional connectivity in term-born infants scanned at 37.5-42.5 weeks PMA, grouped into weekly bins by PMA at scan. Within each bin 20 subjects with the lowest postnatal age at time of scan were selected. Example axial slices for meaningful spatial patterns in primary (A) and association (B) RSNs are shown, overlaid on a T1 structural template and displayed in radiological convention. Results were thresholded at $p < 0.05$ (FWE corrected).

To further quantify longitudinal changes in within-network functional connectivity, we analysed the relationship between PMA at scan and a derived parameter we term ‘core network strength’, defined as the mean β parameter value in each subject’s RSN-specific spatial map (the outputs of stage two of dual regression) after masking by the corresponding group-ICA network template thresholded at $Z > 3$. Three RSNs showed a positive partial correlation between PMA at scan and core network strength (**Fig. 4**). There were no RSNs with negative correlation.

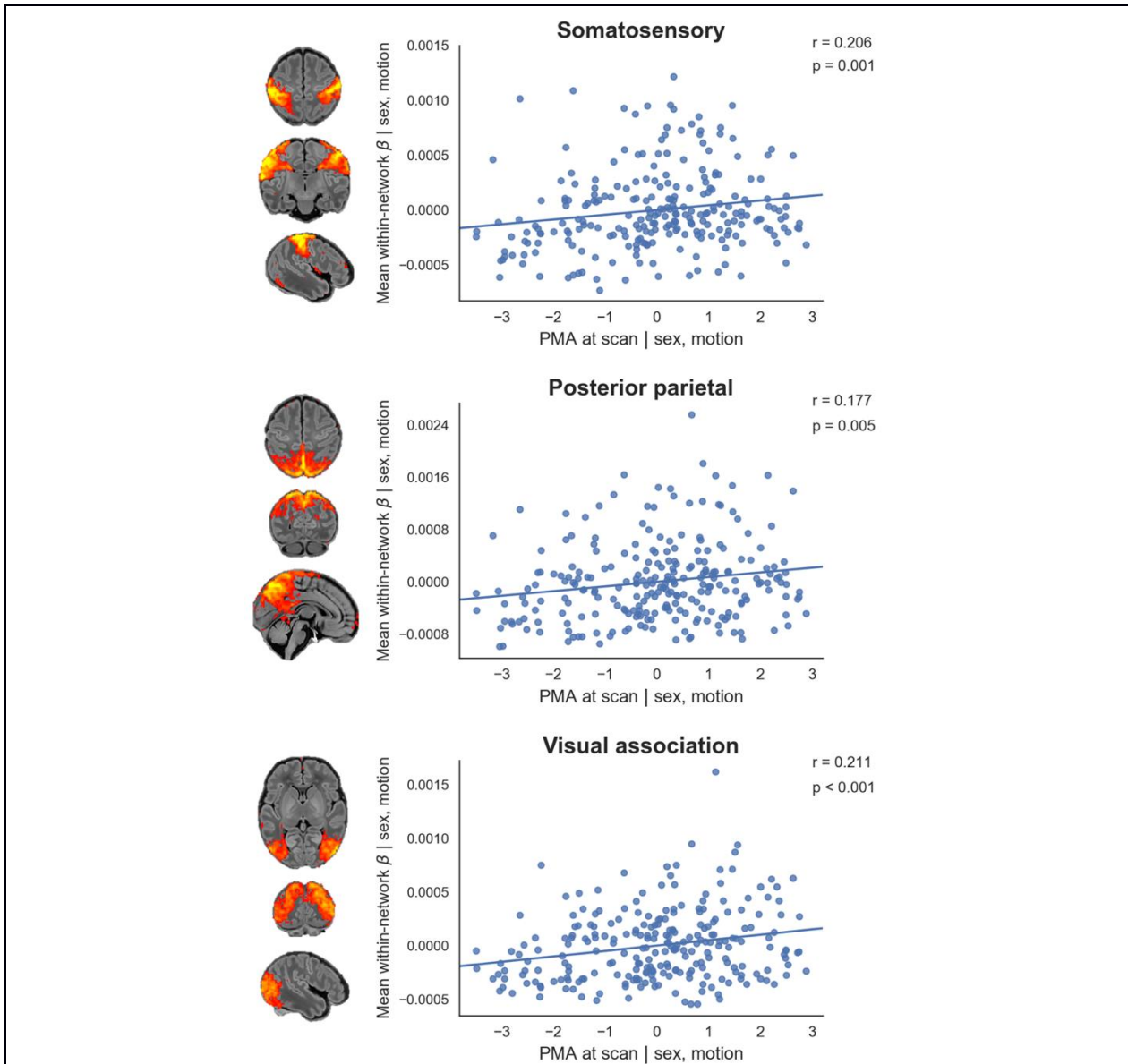


Figure 4. Relationship between postmenstrual age at scan and core network strength. Relationship between the residuals (after correcting for sex and motion) for PMA at scan and core network strength in term-born infants scanned at 37-43.5 weeks PMA. Core network strength was defined as the mean β parameter value in each subject’s RSN-specific spatial map after masking by the corresponding group-ICA network template thresholded at $Z > 3$. Partial Spearman’s correlation coefficients and associated p values are displayed for the three RSNs significant at $p < 0.025$. Example axial, coronal and sagittal slices for meaningful spatial patterns in the corresponding group-ICA network templates are shown for reference.

Effect of Sex

To determine differences in functional connectivity between male and female infants we analysed this as a group effect, while controlling for GA at birth, PMA at scan and motion. Female infants showed increased connectivity of inferior occipito-temporal regions (including the posterior fusiform gyrus) within the visual association network (**Fig. 5**; Bonferroni-corrected, **Supplementary Fig. S3**).

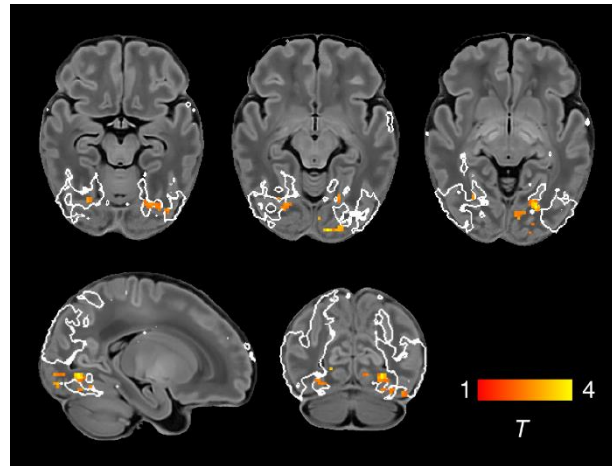


Figure 5. Increased functional connectivity in the visual association network in female infants. Brain regions showing increased functional connectivity within the visual association RSN in female infants. Example axial, sagittal and coronal slices for meaningful spatial patterns are shown, overlaid on a T1 structural template and displayed in radiological convention. T-statistic maps were thresholded at $p < 0.025$ (FWE corrected). White lines represent the outline of the group-ICA visual association network, thresholded at $Z > 3$.

Effect of preterm birth

To determine differences in functional connectivity between term- and preterm-born infants we first analysed this as a group effect, while controlling for PMA at scan, sex and motion. There was extensive impairment of functional connectivity across all RSNs in preterm-born infants; uncorrected core network strength was 23-41% reduced relative to term-born infants across the 11 networks (all $p < 0.001$, independent samples t-tests). Conversely, preterm-born infants showed increased connectivity of the bilateral superior parietal lobule within the lateral motor network (**Fig. 6**; Bonferroni-corrected, **Supplementary Fig. S4**). The association of younger GA at birth with impaired functional connectivity was replicated across all networks in a separate analysis in which GA at birth was entered as a continuous variable, indicating a dose-dependent effect of prematurity on functional connectivity (**Supplementary Fig. S5**; Bonferroni-corrected, **Supplementary Fig. S6**).

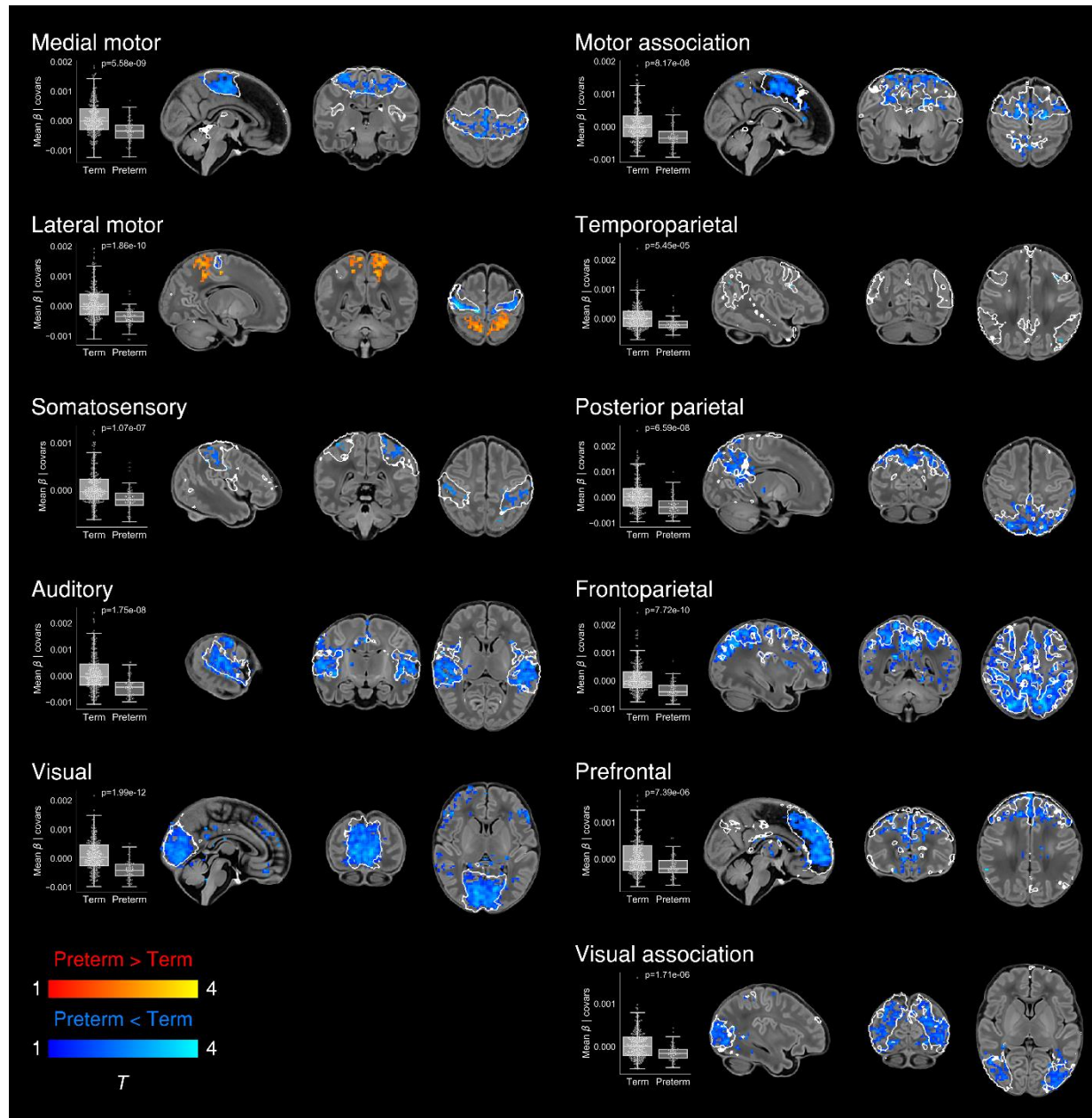


Figure 6. Effect of preterm birth on functional connectivity. Group differences in functional connectivity between term- and preterm-born infants scanned at 37-43.5 weeks PMA. Coloured t -statistic maps thresholded at $p < 0.025$ (FWE corrected) show brain regions with reduced (blue) or increased (red-yellow) connectivity in preterm-born infants. Example sagittal, coronal, and axial slices for meaningful spatial patterns within each RSN are shown, overlaid on a T1 structural template and displayed in radiological convention. White lines represent the outlines of the group-ICA RSNs, thresholded at $Z > 3$. Boxplots show group differences in core network strength after regressing out PMA at scan, sex and motion. Core network strength was defined as the mean β parameter value in each subject's RSN-specific spatial map after masking by the corresponding group-ICA network template thresholded at $Z > 3$. P-values relate to the term vs. preterm group contrast in a GLM in which core network strength was the dependent variable and PMA at scan, sex and motion were controlled for as nuisance covariates.

Discussion

In this large cohort of newborn infants we provide detailed characterization of the maturational trajectories of normal functional network development at TEA, and show that the early developmental disruption imposed by preterm birth is associated with significant and widespread alterations in functional connectivity.

Network architecture and maturation in term-born infants

Overall we find a robust, modular, symmetrical functional organisation of the brain at TEA. Our results confirm and further elucidate the primary-to-higher-order maturational sequence of RSN development. Using a whole-brain, voxel-level approach we depicted changes in the posterior parietal, frontoparietal, prefrontal and visual association networks, showing expansions in network shape with increasing age at scan (Fig. 2). We also investigated the effect of age at scan across a predefined area (the core region, as defined by the template network), demonstrating global changes in network strength or integrity in the somatosensory, posterior parietal and visual association networks (Fig. 4).

Primary networks

We identified five primary RSNs (**Fig. 1A**) which showed adult-like topology from the earliest ages studied (**Fig. 3A**) and no significant change in architecture from 37-43.5 weeks PMA. Primary, unimodal RSNs mature earlier than higher-order networks in the preterm brain (Doria et al., 2010; Liu et al., 2008; Smyser et al., 2010); our finding of an adult-like configuration of primary RSNs at TEA is in agreement with previous studies at this age (Doria et al., 2010; Fransson et al., 2011; Fransson et al., 2009; Fransson et al., 2007; Gao et al., 2014; Gao et al., 2015; Smyser et al., 2010). The precise localisation of sensorimotor networks along the central sulcus is especially striking in our data, even in the youngest infants studied (**Fig. 3A**). Determination of somatotopic maps in primary sensorimotor cortical areas occurs as early as mid-third trimester equivalent age, with similar stimulation response to adults observed by TEA (Allievi et al., 2015; Dall’Orso et al., 2018). We additionally observed a significant increase in core network strength within the somatosensory network from 37-43.5 weeks PMA (**Fig. 4**), possibly reflecting increasing integration of secondary somatosensory cortex at this age (Allievi et al., 2015), and/or increased influence of ex-utero experience on this network. The bilateral insula (**Fig. 1A**) and thalamus (**Supplementary Fig. S1C**) were strongly connected within the medial motor network, consistent with previous studies finding strong

thalamocortical connectivity in sensorimotor networks (Smyser et al., 2016; Toulmin et al., 2015).

Association networks

We identified six RSNs representing higher-order association networks (**Fig. 1C**). Using quantitative (**Fig. 2, Fig. 4**) and qualitative (**Fig. 3**) methods, we found modest expansions in both the spatial extent and core temporal coherence of higher-order association networks from 37-43.5 weeks PMA. To our knowledge this is the first time these changes have been quantified over this brief but developmentally critical period. The heterogeneous timing of functional network development, in which primary networks mature earlier than higher-order association networks, can be related to parallel changes in brain structure (reviewed in Keunen et al., 2017). Structural connectivity of the cortex begins with thalamic connections to frontal, auditory, visual and somatosensory cortices at 24-32 weeks gestation, while long-range cortico-cortical connections are not established until 33-35 weeks (reviewed in Dubois et al., 2016; Kostovic and Jovanov-Milosevic, 2006). The same sequence is later repeated in cortical myelination, with the “primordial” sensorimotor and visual cortices histologically more mature at the time of birth (Flechsig, 1901). White matter tracts connecting to these regions, such as the corticospinal tract and optic radiation, are also the first to mature later in infancy (reviewed in Dubois et al., 2014). The structural and functional ontogeny mirrors the observed behavioural sequence of developmental ‘milestones’ in young children, in which sensorimotor, auditory and visual competencies are acquired before higher-order cognitive functions (Keunen et al., 2017).

The two RSNs showing greatest increase in intrinsic connectivity (core network strength) from 37-43.5 weeks PMA were the posterior parietal network and visual association network (**Fig. 4**). The former encompasses the medial precuneus and posterior cingulate cortices (**Supplementary Fig. S1C**), an area of emerging functional connectivity at TEA (Gao et al., 2009). In adulthood these regions are a prominent component of the DMN, leading some to label infant RSNs encompassing these as DMN precursors (Doria et al., 2010; Fransson et al., 2009; Fransson et al., 2007; Smyser et al., 2010; Smyser et al., 2016). However, the mature DMN also incorporates distinct modules in the anterior cingulate/medial prefrontal cortex, orbitofrontal cortex, lateral temporal cortex and hippocampus (reviewed in Raichle, 2015). We observe no temporal involvement in the posterior parietal network, and only sparse frontal involvement, specifically at the right anterior cingulate (**Supplementary Fig. S1C**) and bilateral orbitofrontal cortex (**Supplementary Fig. S1E**). This dominant posterior hub with limited frontoparietal connectivity bears more similarity to the adult DMN under anaesthesia

(Amico et al., 2014; Bonhomme et al., 2016). Overall we find support for the concept of fragmented local modules prevailing over long-range integration at this period of development, preceding the emergence of a full analogue of the adult DMN at 6-12 months of age (Gao et al., 2014; Gao et al., 2015; Gao et al., 2009).

The visual association network comprises lateral occipital (**Supplementary Fig. S1D**) and inferotemporal (**Supplementary Fig. S1B**) cortices; regions which contribute to the ventral stream of visual processing, in which simple features coded by primary visual cortex are transformed into higher-level representations of objects, invariant of their size, rotation and position, enabling downstream object recognition and semantic processing (DiCarlo et al., 2012; Goodale and Milner, 1992). It was therefore not surprising to find significant growth in the strength of this network from 37-43.5 weeks PMA (**Fig. 2, Fig. 4**), a period in which infants are increasingly exposed to, and able to resolve, objects in the visual field (Dubowitz et al., 1983). Furthermore, after controlling for differences in age, we found areas of increased connectivity within this network in female infants across inferotemporal regions including the posterior fusiform gyrus (**Fig. 5**). The fusiform is sensitive to complex visual stimuli including faces and facial expressions (Li et al., 2019); in the corresponding region of the macaque brain the code determining face cell firing was recently deciphered (Chang and Tsao, 2017). In humans, reduced functional connectivity of the fusiform face area is associated with developmental prosopagnosia (Lohse et al., 2016). The sex difference in functional connectivity we have identified in this region is especially interesting in the context of behavioural data in which female neonates, compared to males, show increased preference for looking at faces (Connellan et al., 2000). Sex differences in visual attention to social stimuli have also been described in older infants (Alexander et al., 2009) and in other newborn primates (Simpson et al., 2016). Structural brain development is sexually dimorphic, with small differences in tissue morphometry observed across the lifespan, frequently involving the temporal lobes, and under the influence of fetal testosterone in males (Lombardo et al., 2012; Studholme et al., 2020). Our finding of a sex difference in functional brain development in the inferior temporal lobes is interesting in this context, although the biological mechanisms for this and any correlations with behavioural data remain unknown at this time. Further investigation of functional connectivity in the ventral stream and social-cognitive development might elucidate mechanisms for sex differences in this domain.

Two RSNs comprised segregated (i.e. non-contiguous) brain regions revealing anatomically meaningful patterns of functional connectivity. The temporoparietal network (**Fig. 1D**) connects a posterior module encompassing the extended Wernicke's area to a smaller anterior module corresponding to Broca's area. Integrated structural-functional analysis in adults

showed this network is facilitated by the arcuate fasciculus (O'Muircheartaigh and Jbabdi, 2018). The instatement of a putative 'language network' in early infancy is supported by stimulus-fMRI showing activation of these regions in response to speech (Dehaene-Lambertz et al., 2002; Dehaene-Lambertz et al., 2006). The frontoparietal network (**Fig. 1B**) connects the frontal, supplementary and parietal eye fields, with close resemblance to the adult dorsal attention network (Vossel et al., 2014). Ocular control relies on widespread white-matter connections between cortical and subcortical regions, the microstructural integrity of which correlates with visual fixation behaviour in the neonate (Stjerna et al., 2015). Striatal projections of the frontal and supplementary eye fields converge upon the caudate nucleus (Parthasarathy et al., 1992); we found a positive association between older PMA at scan and functional connectivity of the caudate nucleus within this frontoparietal network (**Fig. 2**), consistent with active development of the oculomotor corticostriatal system at this age.

Impact of preterm birth

Preterm birth confers a high risk of neurodevelopmental impairment (Bhutta et al., 2002; Marlow et al., 2005; Saigal and Doyle, 2008) and psychiatric illness in later life (Nosarti et al., 2012). Pervasive deficiencies and delays in structural brain maturation have been identified in preterm infants scanned at TEA, even in those without focal brain injury, including macrostructural differences in tissue volume and gyrification (Ball et al., 2012; Kapellou et al., 2006; Keunen et al., 2012; Shimony et al., 2016) and microstructural alterations in both grey and white matter (Ball et al., 2013b; Bouyssi-Kobar et al., 2018a; Krishnan et al., 2007). The overall structural network architecture appears unchanged, with preservation or even abnormal strengthening of the rich-club organisation of highly connected cortical hubs, at the expense of diminished peripheral connectivity and specific disruptions to thalamocortical, cortical-subcortical and short-distance corticocortical connectivity (Ball et al., 2014; Ball et al., 2013a; Ball et al., 2015; Batalle et al., 2017; Lee et al., 2019).

Widespread impairment of functional connectivity

Now we show that, similar to structural connectivity, functional connectivity is profoundly affected by preterm birth. We found striking deficiencies in within-network connectivity across the full range of RSNs studied (**Fig. 6**), also replicated as a dose-dependent relationship, such that increased exposure to prematurity (younger GA at birth) was associated with decreased functional connectivity (**Supplementary Fig. S5**); effects we were not powered to detect in a prior study due to a limited number of term-born infants (Doria *et al.*, 2010). Our results

suggest that although functional connectivity increases across the preterm period (Cao et al., 2016; Doria et al., 2010; Smyser et al., 2010; Smyser et al., 2016; van den Heuvel et al., 2015), it does not reach a normal configuration at TEA. Instead there appears to be an aberrant developmental trajectory, in which connections between brain regions are reconfigured by premature exposure to the extrauterine environment. Graph theoretical approaches have shown global network measures of clustering, integration and modularity at TEA are all reduced in preterm infants compared to full-term controls (Bouyssi-Kobar et al., 2019; Scheinost et al., 2016). Hypothesis-driven seed-based approaches have identified disrupted thalamocortical connectivity (Smyser et al., 2010; Toulmin et al., 2015), consistent with structural disruption of the same (Ball et al., 2015). In our data-driven, whole-brain ICA approach, the main finding was globally reduced within-network functional connectivity. Primary and association RSNs appeared to be similarly affected, in contrast to the findings of Smyser and colleagues, who also employed whole-brain correlation mapping, and found primary RSNs were less affected by prematurity (Smyser et al., 2016). This discrepancy may be due to differences in approach to RSN definition (adult-derived RSNs), network mapping (node-based) and inclusion criteria for the preterm group (< 30 weeks GA at birth). In another study investigating preterm-at-term infants with whole-brain ICA, the method comprised identification of 71 nodes by ICA followed by subject-specific network estimation and selection of discriminatory edges between cases and controls using machine-learning classifiers (Ball et al., 2016). Connections to frontal and basal ganglia nodes were overrepresented among the discriminatory edges, indicating altered connectivity in preterm infants. Taken together, these different approaches provide complementary demonstrations of spatially widespread impaired RSN coherence in the preterm-at-term brain.

Modulation of parieto-motor connectivity

In the context of brain-wide deficiencies in functional connectivity in preterm-at-term infants, it was notable that there was also increased functional connectivity of the bilateral superior parietal lobule (Brodmann area 5) within the lateral motor network, both when prematurity was evaluated as a group effect (**Fig. 6**) and as a continuous variable (**Supplementary Fig. S5**). The lateral motor network corresponds approximately to the primary somatotopic regions serving the upper limb, hand and face (**Fig. 1D**). Ex-utero experience during the preterm period strongly influences the development of sensorimotor networks: bilateral functional responses in the perirolandic cortices to stimulation of the wrist increases with postnatal age, even after controlling for GA at birth (Allievi et al., 2015). Interestingly, connectivity with superior parietal regions appears to occur as a feature of normal development in the lateral motor

network in older term-born infants (**Fig. 3A**). Area 5 comprises the somatosensory association cortex which integrates visual and somatosensory inputs to encode limb configuration in space, enabling coordinated movements within the immediate environment (Graziano et al., 2000; Mountcastle et al., 1975). Neural circuits are shaped by experience during critical periods of development; in animal studies, peak plasticity in somatosensory networks occurs earlier than peak plasticity in visual and auditory networks (reviewed in Reh et al., 2020). It is intuitive that connectivity of area 5 with lateral motor cortex could be highly dependent upon ex-utero experience, given the natural constraints upon limb movement and visuomotor integration in utero. We propose therefore that the experience of premature exposure to the extrauterine environment, occurring at a time of heightened sensorimotor plasticity (Staudt, 2010; Arichi *et al.*, 2014; Allievi *et al.*, 2015), modulates the normal development of parieto-motor connectivity and leads to an abnormal increase in connectivity at TEA; while acknowledging this mechanistic account as speculative at the present time.

Previous studies have identified increased functional connectivity of certain primary cortical regions in preterm-at-term infants compared to controls, specifically the lateral postcentral gyrus with the thalamus (Toulmin et al., 2015) and regional connectivity within occipital/visual networks (Bouyssi-Kobar et al., 2018a). This may occur at the expense of connectivity in other brain areas, and can persist into later life; analysis of language networks in preterm children scanned at 12 years of age showed increased connectivity with primary sensorimotor areas, but reduced connectivity with higher-order frontal areas (Schafer et al., 2009). Relatively conserved topology of core structural networks has been reported in preterm-born babies (Batalle et al., 2017), persisting into later childhood and adulthood (Fischi-Gomez et al., 2016; Karolis et al., 2016). Disruption of the normal balance of sensorimotor development may have persisting effects on later motor and cognitive development. In the mature brain, the superior parietal lobule supports not only the smooth execution of motor plans (Simon et al., 2002) but also more abstract visuospatial functions such as mental rotation (Gogos et al., 2010). The aberrant parietal connectivity we have identified at TEA could therefore be a prelude to specific difficulties occurring with high prevalence in preterm children, such as developmental coordination disorder (Caravale et al., 2019; Davis et al., 2007; Dewey et al., 2019; Kashiwagi et al., 2009; Wilson et al., 2017), inattention and intellectual impairment (reviewed in Rogers et al., 2018). Long-term follow up of the study population at school age will be required to confirm this hypothesis.

Limitations

The customised neonatal imaging system for the dHCP includes a close-fitting head coil sized specifically for the neonatal head, thus providing exceptional signal-to-noise at the cortical surface (Hughes et al., 2017). This bias towards surface-proximate sources is compounded by the use of highly accelerated multiband EPI (Fitzgibbon et al., 2020). As such, this has likely resulted in greater sensitivity to detect correlated signal fluctuations in the cerebral cortex compared to deeper sources such as the thalamus, basal ganglia and cerebellum. This may explain the relatively sparse involvement of subcortical regions in the identified RSNs (**Fig. 1A, 1C**). Thalamocortical and cerebellar functional connectivity may be better appreciated with seed-based methods (Herzmann et al., 2018; Toulmin et al., 2015). We also noted sparse involvement of inferior frontotemporal regions, even at $Z > 1$ (**Supplementary Fig. S1B**). The dHCP functional pipeline includes advanced distortion-correction techniques (Fitzgibbon et al., 2020), but some signal loss related to air/tissue and bone/tissue interfaces in this vicinity cannot be fully excluded, and our use of a single phase-encode direction (anterior-posterior) may also compress signal in the frontal regions. However, this sparsity may also reflect biological reality in these brain regions, which are the least myelinated at birth (Flechsig, 1901) and so may be the least able to participate in long-range phase-synchronous activity.

In this study we used a dense sampling strategy at TEA to infer longitudinal change in RSNs, but each infant was scanned on only one occasion. GA at birth and PMA at scan were strongly correlated within the term-born group, which complicates the interpretation of these longitudinal analyses. Furthermore, as some potentially relevant neonatal characteristics such as intracranial volume and postnatal days of life, are intrinsically associated to some of our variables of interest (i.e., postmenstrual age at scan, sex, gestational age at birth), it is difficult to disentangle their relative contributions to our results.

The optimised fMRI dHCP pipeline includes multiple steps to control for motion and physiological confounds, thus minimising data loss. However, while well-fed babies tend to fall asleep during the scan, subject motion is inherently correlated with the arousal and sleep state of the baby, which may have an effect in the reconstructed RSNs (Horovitz et al., 2009). While our stringent control for high motion during the scan will minimise the potential effect of subject differences in arousal and sleep state, the specific measure that should be used as a surrogate to model arousal state is unclear. Future studies using simultaneous EEG-fMRI could help to better understand the effect of different sleep states on RSNs. Differences in arousal in the scanner between infants and adults should also be considered when comparing RSN topology between these groups (Mitra et al., 2017). Our use of infants scanned at 43.5-44.5 PMA to define the group-ICA components may have missed some sources of structured noise

occurring predominantly at younger ages, such as CSF signal in the cavum septum pellucidum. More fundamentally, the extent to which BOLD signal might be confounded by cerebrovascular factors differing between preterm- and term-born infants (Bouyssi-Kobar et al., 2018b) remains open to debate. Some of the spatial expansions in association RSNs depicted in **Fig. 2** were localised to white matter (see **Supplementary Table S1**), which may also reflect maturational changes in cerebrovascular factors, combined with other age-related changes in sulcal depth and white matter signal to noise ratio. Some of the important temporal dynamics in functional networks may be missed by rs-fMRI, which predominantly identifies activity at $< 0.1\text{Hz}$ (Cordes et al., 2001). Complementary approaches such as EEG may help to address this (Arichi et al., 2017; Mehrkanoon, 2019).

Conclusion

Brain development occurs in a pre-programmed and spatially heterogeneous progression, modulated by environmental influence. As such, we observed different trajectories for different neural systems, obeying a generally primary-to-higher-order sequence of maturation. At TEA we find already instated a complete set of adult-analogous unimodal RSNs corresponding to primary sensorimotor, visual and auditory cortices, with relatively little change from 37-43.5 weeks PMA. In contrast, association RSNs appear fragmented and incomplete compared to the adult repertoire, and are undergoing active maturation at this time. Connectivity within the visual association network in particular is highly associated with age, likely as a result of postnatal environmental experience, but also modified by the sex of the infant. Preterm birth is associated with profoundly reduced functional connectivity across all RSNs, but also with augmentation of parieto-motor connectivity, with possible implications for understanding certain neurocognitive sequelae of prematurity. In future we may be able to positively modulate RSN development in prematurity via targeted environmental manipulations (Lordier et al., 2019). Preterm birth is best conceptualised as a developmental perturbation which reconfigures, rather than simply diminishes, the organisation of functional brain networks.

Acknowledgements

We thank Shona Falconer, Andrew Chew and Nicholas Harper for providing the Bayley-III developmental follow-up data.

Funding

This work was supported by the European Research Council under the European Union Seventh Framework Programme (FP/2007-2013)/ERC Grant Agreement no. 319456. The authors acknowledge infrastructure support from the National Institute for Health Research (NIHR) Mental Health Biomedical Research Centre (BRC) at South London, Maudsley NHS Foundation Trust, King's College London and the NIHR-BRC at Guys and St Thomas' Hospitals NHS Foundation Trust (GSTFT). The authors also acknowledge support in part from the Wellcome Engineering and Physical Sciences Research Council (EPSRC) Centre for Medical Engineering at King's College London [WT 203148/Z/16/Z] and the Medical Research Council (UK) [MR/K006355/1 and MR/L011530/1]. Additional sources of support included the Sackler Institute for Translational Neurodevelopment at King's College London, the European Autism Interventions (EU-AIMS) trial and the EU AIMS-2-TRIALS, a European Innovative Medicines Initiative Joint Undertaking under Grant Agreements No. 115300 and 777394, the resources of which are composed of financial contributions from the European Union's Seventh Framework Programme (Grant FP7/2007–2013). ME was supported by the NIHR-BRC at GSTFT. TA was supported by a Medical Research Council (MRC) Clinician Scientist Fellowship [MR/P008712/1]. JOM and DE received support from the Medical Research Council Centre for Neurodevelopmental Disorders, King's College London [MR/N026063/1]. JOM is supported by a Sir Henry Dale Fellowship jointly funded by the Wellcome Trust and the Royal Society [206675/Z/17/Z]. DB received support from a Wellcome Trust Seed Award in Science [217316/Z/19/Z]. The views expressed are those of the author(s) and not necessarily those of the NHS, the NIHR or the Department of Health. The funders had no role in the design and conduct of the study; collection, management, analysis, and interpretation of the data; preparation, review, or approval of the manuscript; and decision to submit the manuscript for publication.

Figure Legends

Figure 1. Resting-state networks identified by group independent component analysis.

Spontaneous BOLD activity patterns (RSNs) derived from group ICA in 24 term-born infants scanned at 43.5–44.5 weeks PMA. Panels: Example axial, coronal, and sagittal slices for meaningful spatial patterns in primary (A) and association (C) RSNs, thresholded at $Z > 3$ and overlaid on a T1 structural template, displayed in radiological convention. Centre: Functional parcellation of the brain using a 'winner-takes-all' approach based on the RSNs from group ICA. RSNs were spatially smoothed and thresholded at $Z > 1$ prior to determination of the

‘winning’ RSN at each voxel. The resulting volume was projected to the midthickness cortical surface using enclosed (nearest neighbour) volume-to-surface mapping, here displayed on the pial surface of an individual subject scanned at 42 weeks PMA and viewed from the dorsal (B) and left lateral (D) aspects.

Figure 2. Changes in network shape with increasing age at scan. Brain regions showing increasing functional connectivity with older PMA at scan in term-born infants scanned at 37-43.5 weeks PMA. Example sagittal, coronal, and axial slices for meaningful spatial patterns in four RSNs are shown, overlaid on a T1 structural template and displayed in radiological convention. T-statistic maps were thresholded at $p < 0.025$ (FWE corrected). White lines represent the outlines of the group-ICA RSNs, thresholded at $Z > 3$.

Figure 3. Weekly maturation in functional network structure at term-equivalent age. Group-average t-statistic maps of functional connectivity in term-born infants scanned at 37.5-42.5 weeks PMA, grouped into weekly bins by PMA at scan. Within each bin 20 subjects with the lowest postnatal age at time of scan were selected. Example axial slices for meaningful spatial patterns in primary (A) and association (B) RSNs are shown, overlaid on a T1 structural template and displayed in radiological convention. Results were thresholded at $p < 0.05$ (FWE corrected).

Figure 4. Relationship between postmenstrual age at scan and core network strength. Relationship between the residuals (after correcting for sex and motion) for PMA at scan and core network strength in term-born infants scanned at 37-43.5 weeks PMA. Core network strength was defined as the mean β parameter value in each subject’s RSN-specific spatial map after masking by the corresponding group-ICA network template thresholded at $Z > 3$. Partial Spearman’s correlation coefficients and associated p values are displayed for the three RSNs significant at $p < 0.025$. Example axial, coronal and sagittal slices for meaningful spatial patterns in the corresponding group-ICA network templates are shown for reference.

Figure 5. Increased functional connectivity in the visual association network in female infants. Brain regions showing increased functional connectivity within the visual association RSN in female infants. Example axial, sagittal and coronal slices for meaningful spatial patterns are shown, overlaid on a T1 structural template and displayed in radiological convention. T-statistic maps were thresholded at $p < 0.025$ (FWE corrected). White lines represent the outline of the group-ICA visual association network, thresholded at $Z > 3$.

Figure 6. Effect of preterm birth on functional connectivity. Group differences in functional connectivity between term- and preterm-born infants scanned at 37-43.5 weeks PMA. Coloured t-statistic maps thresholded at $p < 0.025$ (FWE corrected) show brain regions with

reduced (blue) or increased (red-yellow) connectivity in preterm-born infants. Example sagittal, coronal, and axial slices for meaningful spatial patterns within each RSN are shown, overlaid on a T1 structural template and displayed in radiological convention. White lines represent the outlines of the group-ICA RSNs, thresholded at $Z > 3$. Boxplots show group differences in core network strength after regressing out PMA at scan, sex and motion. Core network strength was defined as the mean β parameter value in each subject's RSN-specific spatial map after masking by the corresponding group-ICA network template thresholded at $Z > 3$. P-values relate to the term vs. preterm group contrast in a GLM in which core network strength was the dependent variable and PMA at scan, sex and motion were controlled for as nuisance covariates.

Supplementary Figure S1. Spontaneous BOLD activity patterns (RSNs) derived from group ICA in 24 term-born infants scanned at 43.5-44.5 weeks PMA. RSN are expressed as a functional parcellation of the brain using a 'winner-takes-all' approach based on the RSNs from group ICA. RSNs were spatially smoothed and thresholded at $Z > 1$ prior to determination of the 'winning' RSN at each voxel. The resulting volume was projected to the midthickness cortical surface using enclosed (nearest neighbour) volume-to-surface mapping, here displayed on the pial surface of an individual subject scanned at 42 weeks PMA and viewed from the superior (A), inferior (B), medial (C), lateral (D), anterior (D) and posterior (E) aspects.

Supplementary Figure S2. Changes in network shape with increasing age at scan (Bonferroni-corrected). Brain regions showing increased functional connectivity with older PMA at scan in term-born infants scanned at 37-43.5 weeks PMA. Example sagittal, coronal, and axial slices for meaningful spatial patterns in four RSNs are shown, overlaid on a T1 structural template and displayed in radiological convention. T-statistic maps were thresholded at $p < 0.025/11$ (i.e. $p < 0.002$) (FWE corrected). White lines represent the outlines of the group-ICA RSNs, thresholded at $Z > 3$.

Supplementary Figure S3. Increased functional connectivity in the visual association network in female infants (Bonferroni-corrected). Brain regions showing increased functional connectivity within the visual association RSN in female infants. Example axial, sagittal and coronal slices for meaningful spatial patterns are shown, overlaid on a T1 structural template and displayed in radiological convention. T-statistic maps were thresholded at $p < 0.025/11$ (i.e. $p < 0.002$) (FWE corrected). White lines represent the outline of the group-ICA visual association network, thresholded at $Z > 3$.

Supplementary Figure S4. Effect of preterm birth on functional connectivity (Bonferroni-corrected). Group differences in functional connectivity between term- and preterm-born

infants scanned at 37-43.5 weeks PMA. Coloured t-statistic maps thresholded at $p < 0.025/11$ (i.e. $p < 0.002$) (FWE corrected) show brain regions with reduced (blue) or increased (red-yellow) connectivity in preterm-born infants. Example sagittal, coronal, and axial slices for meaningful spatial patterns within each RSN are shown, overlaid on a T1 structural template and displayed in radiological convention. White lines represent the outlines of the group-ICA RSNs, thresholded at $Z > 3$.

Supplementary Figure S5. Effect of gestational age at birth on functional connectivity.

Association of functional connectivity and gestational age at birth (GA) in term- and preterm-born infants scanned at 37-43.5 weeks PMA. Coloured t-statistic maps thresholded at $p < 0.025$ (FWE corrected) show connectivity in brain regions negatively (blue) or positively (red-yellow) associated with gestational age at birth. Example sagittal, coronal, and axial slices for meaningful spatial patterns within each RSN are shown, overlaid on a T1 structural template and displayed in radiological convention. White lines represent the outlines of the group-ICA RSNs, thresholded at $Z > 3$.

Supplementary Figure S6. Effect of gestational age at birth on functional connectivity

(Bonferroni-corrected). Association of functional connectivity and gestational age at birth (GA) in term- and preterm-born infants scanned at 37-43.5 weeks PMA. Coloured t-statistic maps thresholded at $p < 0.025/11$ (i.e. $p < 0.002$) (FWE corrected) show connectivity in brain regions negatively (blue) or positively (red-yellow) associated with gestational age at birth. Example sagittal, coronal, and axial slices for meaningful spatial patterns within each RSN are shown, overlaid on a T1 structural template and displayed in radiological convention. White lines represent the outlines of the group-ICA RSNs, thresholded at $Z > 3$.

References

- Alexander GM, Wilcox T, Woods R. Sex Differences in Infants' Visual Interest in Toys. *Archives of Sexual Behaviour* 2009; 38: 427-433.
- Allievi AG, Arichi T, Tusor N, Kimpton J, Arulkumaran S, Counsell SJ, *et al.* Maturation of Sensori-Motor Functional Responses in the Preterm Brain. *Cerebral Cortex* 2015; 26(1): 402-13.
- Amico E, Gomez F, Di Perri C, Vanhaudenhuyse A, Lesenfants D, Boveroux P, *et al.* Posterior Cingulate Cortex-Related Co-Activation Patterns: A Resting State fMRI Study in Propofol-Induced Loss of Consciousness. *PloS one* 2014; 9(6): e100012.
- Andersson JLR, Graham MS, Drobnjak I, Zhang H, Campbell J. Susceptibility-induced distortion that varies due to motion: Correction in diffusion MR without acquiring additional data. *NeuroImage* 2018; 171: 277-95.

- Andersson JLR, Graham MS, Drobniak I, Zhang H, Filippini N, Bastiani M. Towards a comprehensive framework for movement and distortion correction of diffusion MR images: Within volume movement. *NeuroImage* 2017; 152: 450-66.
- Andersson JLR, Hutton C, Ashburner J, Turner R, Friston K. Modeling Geometric Deformations in EPI Time Series. *NeuroImage* 2001; 13(5): 903-19.
- Andersson JLR, Skare S, Ashburner J. How to correct susceptibility distortions in spin-echo echo-planar images: application to diffusion tensor imaging. *NeuroImage* 2003; 20(2): 870-88.
- Arichi T, Counsell SJ, Allievi AG, Chew AT, Martinez-Biarge M, Mondì V, *et al.* The effects of hemorrhagic parenchymal infarction on the establishment of sensori-motor structural and functional connectivity in early infancy. *Neuroradiology* 2014; 56(11): 985-94.
- Arichi T, Whitehead K, Barone G, Pressler R, Padormo F, Edwards AD, *et al.* Localization of spontaneous bursting neuronal activity in the preterm human brain with simultaneous EEG-fMRI. *eLife* 2017; 6: e27814.
- Avants BB, Epstein CL, Grossman M, Gee JC. Symmetric diffeomorphic image registration with cross-correlation: Evaluating automated labeling of elderly and neurodegenerative brain. *Medical Image Analysis* 2008; 12(1): 26-41.
- Ball G, Aljabar P, Arichi T, Tusor N, Cox D, Merchant N, *et al.* Machine-learning to characterise neonatal functional connectivity in the preterm brain. *NeuroImage* 2016; 124(Pt A): 267-75.
- Ball G, Aljabar P, Zebari S, Tusor N, Arichi T, Merchant N, *et al.* Rich-club organization of the newborn human brain. *Proceedings of the National Academy of Sciences* 2014; 111(20): 7456-61.
- Ball G, Boardman JP, Aljabar P, Pandit A, Arichi T, Merchant N, *et al.* The influence of preterm birth on the developing thalamocortical connectome. *Cortex; a journal devoted to the study of the nervous system and behavior* 2013a; 49(6): 1711-21.
- Ball G, Boardman JP, Rueckert D, Aljabar P, Arichi T, Merchant N, *et al.* The effect of preterm birth on thalamic and cortical development. *Cerebral cortex (New York, NY : 1991)* 2012; 22(5): 1016-24.
- Ball G, Pazderova L, Chew A, Tusor N, Merchant N, Arichi T, *et al.* Thalamocortical Connectivity Predicts Cognition in Children Born Preterm. *Cerebral cortex (New York, NY : 1991)* 2015; 25(11): 4310-8.
- Ball G, Srinivasan L, Aljabar P, Counsell SJ, Durighel G, Hajnal JV, *et al.* Development of cortical microstructure in the preterm human brain. *Proceedings of the National Academy of Sciences* 2013b; 110(23): 9541-6.
- Batalle D, Hughes EJ, Zhang H, Tournier JD, Tusor N, Aljabar P, *et al.* Early development of structural networks and the impact of prematurity on brain connectivity. *NeuroImage* 2017; 149: 379-92.
- Beckmann CF, Mackay CE, Filippini N, Smith SM. Group comparison of resting-state FMRI data using multi-subject ICA and dual regression. *Organisation for Human Brain Mapping. San Francisco*; 2009.
- Beckmann CF, Smith SM. Probabilistic independent component analysis for functional magnetic resonance imaging. *IEEE transactions on medical imaging* 2004; 23(2): 137-52.
- Bhutta AT, Cleves MA, Casey PH, Cradock MM, Anand KJ. Cognitive and behavioral outcomes of school-aged children who were born preterm: a meta-analysis. *Jama* 2002; 288(6): 728-37.
- Biswal B, Yetkin FZ, Haughton VM, Hyde JS. Functional connectivity in the motor cortex of resting human brain using echo-planar MRI. *Magnetic resonance in medicine* 1995; 34(4): 537-41.
- Blankenship AG, Feller MB. Mechanisms underlying spontaneous patterned activity in developing neural circuits. *Nature reviews Neuroscience* 2010; 11(1): 18-29.

- Bonhomme V, Vanhaudenhuyse A, Demertzi A, Bruno MA, Jaquet O, Bahri MA, *et al.* Resting-state Network-specific Breakdown of Functional Connectivity during Ketamine Alteration of Consciousness in Volunteers. *Anesthesiology* 2016; 125(5): 873-88.
- Bouyssi-Kobar M, Brossard-Racine M, Jacobs M, Murnick J, Chang T, Limperopoulos C. Regional microstructural organization of the cerebral cortex is affected by preterm birth. *NeuroImage Clinical* 2018a; 18: 871-80.
- Bouyssi-Kobar M, De Asis-Cruz J, Murnick J, Chang T, Limperopoulos C. Altered Functional Brain Network Integration, Segregation, and Modularity in Infants Born Very Preterm at Term-Equivalent Age. *J Pediatr* 2019; 213: 13-21.e1.
- Bouyssi-Kobar M, Murnick J, Brossard-Racine M, Chang T, Mahdi E, Jacobs M, *et al.* Altered Cerebral Perfusion in Infants Born Preterm Compared with Infants Born Full Term. *The Journal of Pediatrics* 2018b; 193: 54-61.e2.
- Broström L, Bolk J, Padilla N, Skiöld B, Eklöf E, Mårtensson G, *et al.* Clinical Implications of Diffuse Excessive High Signal Intensity (DEHSI) on Neonatal MRI in School Age Children Born Extremely Preterm. *PLoS One* 2016; 11(2): e0149578.
- Cao M, He Y, Dai Z, Liao X, Jeon T, Ouyang M, *et al.* Early Development of Functional Network Segregation Revealed by Connectomic Analysis of the Preterm Human Brain. *Cerebral Cortex* 2016; 27(3): 1949-63.
- Caravale B, Herich L, Zoia S, Capone L, Voller F, Carrozzi M, *et al.* Risk of Developmental Coordination Disorder in Italian very preterm children at school age compared to general population controls. *European journal of paediatric neurology : EJPN : official journal of the European Paediatric Neurology Society* 2019; 23(2): 296-303.
- Chang L, Tsao DY. The Code for Facial Identity in the Primate Brain. *Cell* 2017; 169(6): 1013-28.e14.
- Ciarrusta J, O'Muircheartaigh J, Dimitrova R, Batalle D, Cordero-Grande L, Price A, *et al.* Social Brain Functional Maturation in Newborn Infants With and Without a Family History of Autism Spectrum Disorder. *JAMA Network Open* 2019; 2(4): e191868-e.
- Connellan J, Baron-Cohen S, Wheelwright S, Batki A, Ahluwalia J. Sex differences in human neonatal social perception. *Infant Behavior & Development* 2000; 23(1): 113-8.
- Cordes D, Haughton VM, Arfanakis K, Carew JD, Turski PA, Moritz CH, *et al.* Frequencies contributing to functional connectivity in the cerebral cortex in "resting-state" data. *AJNR American journal of neuroradiology* 2001; 22(7): 1326-33.
- Dall'Orso S, Steinweg J, Allievi AG, Edwards AD, Burdet E, Arichi T. Somatotopic Mapping of the Developing Sensorimotor Cortex in the Preterm Human Brain. *Cerebral Cortex* 2018; 28(7): 2507-15.
- Damoiseaux JS, Rombouts SARB, Barkhof F, Scheltens P, Stam CJ, Smith SM, *et al.* Consistent resting-state networks across healthy subjects. *Proceedings of the National Academy of Sciences* 2006; 103(37): 13848-53.
- Davis NM, Ford GW, Anderson PJ, Doyle LW. Developmental coordination disorder at 8 years of age in a regional cohort of extremely-low-birthweight or very preterm infants. *Developmental medicine and child neurology* 2007; 49(5): 325-30.
- De Luca M, Beckmann CF, De Stefano N, Matthews PM, Smith SM. fMRI resting state networks define distinct modes of long-distance interactions in the human brain. *NeuroImage* 2006; 29(4): 1359-67.
- Dehaene-Lambertz G, Dehaene S, Hertz-Pannier L. Functional neuroimaging of speech perception in infants. *Science (New York, NY)* 2002; 298(5600): 2013-5.
- Dehaene-Lambertz G, Hertz-Pannier L, Dubois J, Mériaux S, Roche A, Sigman M, *et al.* Functional organization of perisylvian activation during presentation of sentences in preverbal infants. *Proceedings of the National Academy of Sciences* 2006; 103(38): 14240-5.
- Denisova K. Neurobiology, not artifacts: Challenges and guidelines for imaging the high risk infant. *NeuroImage* 2019; 185: 624-40.
- Dewey D, Thompson DK, Kelly CE, Spittle AJ, Cheong JLY, Doyle LW, *et al.* Very preterm children at risk for developmental coordination disorder have brain alterations in motor areas. *Acta Paediatrica* 2019; 108(9): 1649-60.

- DiCarlo JJ, Zoccolan D, Rust NC. How does the brain solve visual object recognition? *Neuron* 2012; 73(3): 415-34.
- Doria V, Beckmann CF, Arichi T, Merchant N, Groppo M, Turkheimer FE, *et al.* Emergence of resting state networks in the preterm human brain. *Proceedings of the National Academy of Sciences of the United States of America* 2010; 107(46): 20015-20.
- Dubois J, Adibpour P, Poupon C, Hertz-Pannier L, Dehaene-Lambertz G. MRI and M/EEG studies of the White Matter Development in Human Fetuses and Infants: Review and Opinion. *Brain Plast* 2016; 2(1): 49-69.
- Dubois J, Dehaene-Lambertz G, Kulikova S, Poupon C, Huppi PS, Hertz-Pannier L. The early development of brain white matter: a review of imaging studies in fetuses, newborns and infants. *Neuroscience* 2014; 276: 48-71.
- Dubois J, Lefevre J, Angleys H, Leroy F, Fischer C, Lebenberg J, *et al.* The dynamics of cortical folding waves and prematurity-related deviations revealed by spatial and spectral analysis of gyrification. *NeuroImage* 2019; 185: 934-46.
- Dubowitz LM, Mushin J, Morante A, Placzek M. The maturation of visual acuity in neurologically normal and abnormal newborn infants. *Behavioural brain research* 1983; 10(1): 39-45.
- Finn ES, Shen X, Scheinost D, Rosenberg MD, Huang J, Chun MM, *et al.* Functional connectome fingerprinting: identifying individuals using patterns of brain connectivity. *Nature neuroscience* 2015; 18(11): 1664-71.
- Fischi-Gomez E, Muñoz-Moreno E, Vasung L, Griffa A, Borradori-Tolsa C, Monnier M, *et al.* Brain network characterization of high-risk preterm-born school-age children. *NeuroImage: Clinical* 2016; 11: 195-209.
- Fitzgibbon SP, Harrison SJ, Jenkinson M, Baxter L, Robinson EC, Bastiani M, *et al.* The developing Human Connectome Project (dHCP) automated resting-state functional processing framework for newborn infants. *NeuroImage* 2020; 223: 117303.
- Flechsig P. DEVELOPMENTAL (MYELOGENETIC) LOCALISATION OF THE CEREBRAL CORTEX IN THE HUMAN SUBJECT. *The Lancet* 1901; 158(4077): 1027-30.
- Fransson P, Aden U, Blennow M, Lagercrantz H. The functional architecture of the infant brain as revealed by resting-state fMRI. *Cerebral cortex (New York, NY : 1991)* 2011; 21(1): 145-54.
- Fransson P, Skiold B, Engstrom M, Hallberg B, Mosskin M, Aden U, *et al.* Spontaneous brain activity in the newborn brain during natural sleep--an fMRI study in infants born at full term. *Pediatric research* 2009; 66(3): 301-5.
- Fransson P, Skiold B, Horsch S, Nordell A, Blennow M, Lagercrantz H, *et al.* Resting-state networks in the infant brain. *Proceedings of the National Academy of Sciences of the United States of America* 2007; 104(39): 15531-6.
- Gao W, Alcauter S, Elton A, Hernandez-Castillo CR, Smith JK, Ramirez J, *et al.* Functional Network Development During the First Year: Relative Sequence and Socioeconomic Correlations. *Cerebral Cortex* 2014; 25(9): 2919-28.
- Gao W, Alcauter S, Smith JK, Gilmore JH, Lin W. Development of human brain cortical network architecture during infancy. *Brain structure & function* 2015; 220(2): 1173-86.
- Gao W, Zhu H, Giovanello KS, Smith JK, Shen D, Gilmore JH, *et al.* Evidence on the emergence of the brain's default network from 2-week-old to 2-year-old healthy pediatric subjects. *Proceedings of the National Academy of Sciences* 2009; 106(16): 6790-5.
- Glasser MF, Coalson TS, Robinson EC, Hacker CD, Harwell J, Yacoub E, *et al.* A multi-modal parcellation of human cerebral cortex. *Nature* 2016; 536(7615): 171-8.
- Gogos A, Gavrilescu M, Davison S, Searle K, Adams J, Rossell SL, *et al.* Greater superior than inferior parietal lobule activation with increasing rotation angle during mental rotation: an fMRI study. *Neuropsychologia* 2010; 48(2): 529-35.
- Goodale MA, Milner AD. Separate visual pathways for perception and action. *Trends in neurosciences* 1992; 15(1): 20-5.

- Graziano MS, Cooke DF, Taylor CS. Coding the location of the arm by sight. *Science* (New York, NY) 2000; 290(5497): 1782-6.
- Greve DN, Fischl B. Accurate and robust brain image alignment using boundary-based registration. *NeuroImage* 2009; 48(1): 63-72.
- Herzmann CS, Snyder AZ, Kenley JK, Rogers CE, Shimony JS, Smyser CD. Cerebellar Functional Connectivity in Term- and Very Preterm-Born Infants. *Cerebral Cortex* 2018; 29(3): 1174-84.
- Horovitz SG, Braun AR, Carr WS, Picchioni D, Balkin TJ, Fukunaga M, *et al.* Decoupling of the brain's default mode network during deep sleep. *Proceedings of the National Academy of Sciences* 2009; 106(27): 11376-81.
- Hughes EJ, Winchman T, Padormo F, Teixeira R, Wurie J, Sharma M, *et al.* A dedicated neonatal brain imaging system. *Magnetic resonance in medicine* 2017; 78(2): 794-804.
- Kapellou O, Counsell SJ, Kennea N, Dyet L, Saeed N, Stark J, *et al.* Abnormal Cortical Development after Premature Birth Shown by Altered Allometric Scaling of Brain Growth. *PLOS Medicine* 2006; 3(8): e265.
- Karolis VR, Froudust-Walsh S, Brittain PJ, Kroll J, Ball G, Edwards AD, *et al.* Reinforcement of the Brain's Rich-Club Architecture Following Early Neurodevelopmental Disruption Caused by Very Preterm Birth. *Cerebral cortex* (New York, NY : 1991) 2016; 26(3): 1322-35.
- Kashiwagi M, Iwaki S, Narumi Y, Tamai H, Suzuki S. Parietal dysfunction in developmental coordination disorder: a functional MRI study. *Neuroreport* 2009; 20(15): 1319-24.
- Kersbergen KJ, Benders MJNL, Groenendaal F, Koopman-Esseboom C, Nievelstein RAJ, van Haastert IC, *et al.* Different Patterns of Punctate White Matter Lesions in Serially Scanned Preterm Infants. *PLoS One* 2014; 9(10): e108904.
- Keunen K, Counsell SJ, Benders M. The emergence of functional architecture during early brain development. *NeuroImage* 2017; 160: 2-14.
- Keunen K, Kersbergen KJ, Groenendaal F, Isgum I, de Vries LS, Benders MJ. Brain tissue volumes in preterm infants: prematurity, perinatal risk factors and neurodevelopmental outcome: a systematic review. *The journal of maternal-fetal & neonatal medicine : the official journal of the European Association of Perinatal Medicine, the Federation of Asia and Oceania Perinatal Societies, the International Society of Perinatal Obstet* 2012; 25 Suppl 1: 89-100.
- Kostovic I, Jovanov-Milosevic N. The development of cerebral connections during the first 20-45 weeks' gestation. *Seminars in fetal & neonatal medicine* 2006; 11(6): 415-22.
- Krishnan ML, Dyet LE, Boardman JP, Kapellou O, Allsop JM, Cowan F, *et al.* Relationship between white matter apparent diffusion coefficients in preterm infants at term-equivalent age and developmental outcome at 2 years. *Pediatrics* 2007; 120(3): e604-9.
- Lee JY, Park HK, Lee HJ. Accelerated Small-World Property of Structural Brain Networks in Preterm Infants at Term-Equivalent Age. *Neonatology* 2019; 115(2): 99-107.
- Li Y, Richardson RM, Ghuman AS. Posterior Fusiform and Midfusiform Contribute to Distinct Stages of Facial Expression Processing. *Cerebral cortex* (New York, NY : 1991) 2019; 29(7): 3209-19.
- Liu WC, Flax JF, Guise KG, Sukul V, Benasich AA. Functional connectivity of the sensorimotor area in naturally sleeping infants. *Brain research* 2008; 1223: 42-9.
- Lohse M, Garrido L, Driver J, Dolan RJ, Duchaine BC, Furl N. Effective Connectivity from Early Visual Cortex to Posterior Occipitotemporal Face Areas Supports Face Selectivity and Predicts Developmental Prosopagnosia. *The Journal of Neuroscience* 2016; 36(13): 3821-8.
- Lombardo MV, Ashwin E, Auyeung B, Chakrabarti B, Taylor K, Hackett G, *et al.* Fetal Testosterone Influences Sexually Dimorphic Gray Matter in the Human Brain. *The Journal of Neuroscience* 2012; 32(2): 674-680.
- Lordier L, Meskaldji D-E, Grouiller F, Pittet MP, Vollenweider A, Vasung L, *et al.* Music in premature infants enhances high-level cognitive brain networks. *Proceedings of the National Academy of Sciences* 2019; 116(24): 12103-8.

- Marlow N, Wolke D, Bracewell MA, Samara M. Neurologic and Developmental Disability at Six Years of Age after Extremely Preterm Birth. *New England Journal of Medicine* 2005; 352(1): 9-19.
- Mehrkanoon S. Discovering dynamic functional networks in the human neonatal brain with electric source imaging. *bioRxiv* 2019: 545616.
- Mitra A, Snyder AZ, Tagliazucchi E, Laufs H, Elison J, Emerson RW, *et al.* Resting-state fMRI in sleeping infants more closely resembles adult sleep than adult wakefulness. *PloS one* 2017; 12(11): e0188122.
- Mountcastle VB, Lynch JC, Georgopoulos A, Sakata H, Acuna C. Posterior parietal association cortex of the monkey: command functions for operations within extrapersonal space. *Journal of neurophysiology* 1975; 38(4): 871-908.
- Nickerson LD, Smith SM, Öngür D, Beckmann CF. Using Dual Regression to Investigate Network Shape and Amplitude in Functional Connectivity Analyses. *Frontiers in Neuroscience* 2017; 11(115).
- Nosarti C, Reichenberg A, Murray RM, Cnattingius S, Lambe MP, Yin L, *et al.* Preterm birth and psychiatric disorders in young adult life. *Archives of general psychiatry* 2012; 69(6): E1-8.
- O'Muircheartaigh J, Jbabdi S. Concurrent white matter bundles and grey matter networks using independent component analysis. *NeuroImage* 2018; 170: 296-306.
- O'Shea TM, Allred EN, Kuban KCK, Hirtz D, Specter B, Durfee S, *et al.* Intraventricular hemorrhage and developmental outcomes at 24 months of age in extremely preterm infants. *Journal of child neurology* 2012; 27(1): 22-29.
- Parthasarathy H, Schall J, Graybiel A. Distributed but convergent ordering of corticostriatal projections: analysis of the frontal eye field and the supplementary eye field in the macaque monkey. *The Journal of Neuroscience* 1992; 12(11): 4468-88.
- Power JD, Barnes KA, Snyder AZ, Schlaggar BL, Petersen SE. Spurious but systematic correlations in functional connectivity MRI networks arise from subject motion. *NeuroImage* 2012; 59(3): 2142-54.
- Price A, Cordero-Grande L, Malik S, Abaei M, Arichi T, Hughes E, *et al.* Accelerated neonatal fMRI using multiband EPI. *Proceedings of the 23rd Annual Meeting of ISMRM, Toronto, Canada* 2015: 3911.
- Raichle ME. The brain's default mode network. *Annual review of neuroscience* 2015; 38: 433-47.
- Raichle ME, MacLeod AM, Snyder AZ, Powers WJ, Gusnard DA, Shulman GL. A default mode of brain function. *Proceedings of the National Academy of Sciences* 2001; 98(2): 676-82.
- Reh RK, Dias BG, Nelson CA, Kaufer D, Werker JF, Kolb B, *et al.* Critical period regulation across multiple timescales. *Proceedings of the National Academy of Sciences* 2020; 117(38): 23242-51.
- Rogers CE, Lean RE, Wheelock MD, Smyser CD. Aberrant structural and functional connectivity and neurodevelopmental impairment in preterm children. *J Neurodev Disord* 2018; 10(1): 38-.
- Saigal S, Doyle LW. An overview of mortality and sequelae of preterm birth from infancy to adulthood. *Lancet (London, England)* 2008; 371(9608): 261-9.
- Salimi-Khorshidi G, Douaud G, Beckmann CF, Glasser MF, Griffanti L, Smith SM. Automatic denoising of functional MRI data: combining independent component analysis and hierarchical fusion of classifiers. *NeuroImage* 2014; 90: 449-68.
- Satterthwaite TD, Wolf DH, Loughhead J, Ruparel K, Elliott MA, Hakonarson H, *et al.* Impact of in-scanner head motion on multiple measures of functional connectivity: relevance for studies of neurodevelopment in youth. *NeuroImage* 2012; 60(1): 623-32.
- Schafer RJ, Lacadie C, Vohr B, Kesler SR, Katz KH, Schneider KC, *et al.* Alterations in functional connectivity for language in prematurely born adolescents. *Brain : a journal of neurology* 2009; 132(3): 661-70.

- Scheinost D, Kwon SH, Shen X, Lacadie C, Schneider KC, Dai F, *et al.* Preterm birth alters neonatal, functional rich club organization. *Brain structure & function* 2016; 221(6): 3211-22.
- Schuh A, Makropoulos A, Robinson EC, Cordero-Grande L, Hughes E, Hutter J, *et al.* Unbiased construction of a temporally consistent morphological atlas of neonatal brain development. *bioRxiv* 2018: 251512.
- Shi F, Yap P-T, Wu G, Jia H, Gilmore JH, Lin W, *et al.* Infant Brain Atlases from Neonates to 1- and 2-Year-Olds. *PloS one* 2011; 6(4): e18746.
- Shimony JS, Smyser CD, Wideman G, Alexopoulos D, Hill J, Harwell J, *et al.* Comparison of cortical folding measures for evaluation of developing human brain. *NeuroImage* 2016; 125: 780-90.
- Simon O, Mangin JF, Cohen L, Le Bihan D, Dehaene S. Topographical layout of hand, eye, calculation, and language-related areas in the human parietal lobe. *Neuron* 2002; 33(3): 475-87.
- Simpson EA, Nicolini Y, Shetler M, Suomi SJ, Ferrari PF, Paukner A. Experience-independent sex differences in newborn macaques: Females are more social than males. *Scientific Reports* 2016; 6: 19669.
- Smith SM, Nichols TE. Threshold-free cluster enhancement: addressing problems of smoothing, threshold dependence and localisation in cluster inference. *NeuroImage* 2009; 44(1): 83-98.
- Smyser CD, Inder TE, Shimony JS, Hill JE, Degnan AJ, Snyder AZ, *et al.* Longitudinal analysis of neural network development in preterm infants. *Cerebral cortex* (New York, NY : 1991) 2010; 20(12): 2852-62.
- Smyser CD, Snyder AZ, Shimony JS, Mitra A, Inder TE, Neil JJ. Resting-State Network Complexity and Magnitude Are Reduced in Prematurely Born Infants. *Cerebral cortex* (New York, NY : 1991) 2016; 26(1): 322-33.
- Staudt M. Reorganization after pre- and perinatal brain lesions*. *Journal of Anatomy* 2010; 217(4): 469-74.
- Steggerda SJ, de Bruïne FT, van den Berg-Huysmans AA, Rijken M, Leijser LM, Walther FJ, *et al.* Small cerebellar hemorrhage in preterm infants: perinatal and postnatal factors and outcome. *Cerebellum* 2013; 12(6), 794-801.
- Stjerna S, Sairanen V, Gröhn R, Andersson S, Metsäranta M, Lano A, *et al.* Visual Fixation in Human Newborns Correlates with Extensive White Matter Networks and Predicts Long-Term Neurocognitive Development. *The Journal of Neuroscience* 2015; 35(12): 4824-9.
- Studholme C, Kroenke CD, Dighe M. Motion corrected MRI differentiates male and female human brain growth trajectories from mid-gestation. *Nature Communications* 2020; 11: 3038.
- Toulmin H, Beckmann CF, O'Muircheartaigh J, Ball G, Nongena P, Makropoulos A, *et al.* Specialization and integration of functional thalamocortical connectivity in the human infant. *Proceedings of the National Academy of Sciences of the United States of America* 2015; 112(20): 6485-90.
- Tzourio-Mazoyer N, Landeau B, Papathanassiou D, Crivello F, Etard O, Delcroix N, *et al.* Automated anatomical labeling of activations in SPM using a macroscopic anatomical parcellation of the MNI MRI single-subject brain. *NeuroImage* 2002; 15(1): 273-89.
- van den Heuvel MP, Kersbergen KJ, de Reus MA, Keunen K, Kahn RS, Groenendaal F, *et al.* The Neonatal Connectome During Preterm Brain Development. *Cerebral cortex* (New York, NY : 1991) 2015; 25(9): 3000-13.
- Vasung L, Abaci Turk E, Ferradal SL, Sutin J, Stout JN, Ahtam B, *et al.* Exploring early human brain development with structural and physiological neuroimaging. *NeuroImage* 2019; 187: 226-54.
- Vossel S, Geng JJ, Fink GR. Dorsal and ventral attention systems: distinct neural circuits but collaborative roles. *The Neuroscientist : a review journal bringing neurobiology, neurology and psychiatry* 2014; 20(2): 150-9.
- Wang D, Buckner RL, Fox MD, Holt DJ, Holmes AJ, Stoecklein S, *et al.* Parcellating cortical functional networks in individuals. *Nature neuroscience* 2015; 18(12): 1853-60.

- Whitehead K, Laudiano-Dray MP, Meek J, Fabrizi L. Emergence of mature cortical activity in wakefulness and sleep in healthy preterm and full-term infants. *Sleep* 2018; 41(8).
- Wilson PH, Smits-Engelsman B, Caeyenberghs K, Steenbergen B, Sugden D, Clark J, *et al.* Cognitive and neuroimaging findings in developmental coordination disorder: new insights from a systematic review of recent research. *Developmental Medicine & Child Neurology* 2017; 59(11): 1117-29.
- Winkler AM, Ridgway GR, Webster MA, Smith SM, Nichols TE. Permutation inference for the general linear model. *NeuroImage* 2014; 92: 381-97.